




Article

Characteristic Evaluation and Finite Element Analysis of a New Glass Fiber Post Based on Bio-Derived Polybenzoxazine

Phattarin Mora ¹, Sarawut Rimdusit ²  and Chanchira Jubsilp ^{1,*}

¹ Department of Chemical Engineering, Faculty of Engineering, Srinakharinwirot University, Nakhonnayok 26120, Thailand; phattarin@g.swu.ac.th

² Research Unit in Polymeric Materials for Medical Practice Devices, Department of Chemical Engineering, Faculty of Engineering, Chulalongkorn University, Bangkok 10330, Thailand; sarawut.r@chula.ac.th

* Correspondence: chanchira@g.swu.ac.th; Tel.: +66-26-495-000 (ext. 27104-6)

Abstract: A new type of glass fiber (GF)-reinforced bio-derived polybenzoxazine (GF/bio-derived PBz) composites suitable for dental post applications was developed. The study assessed the effects of different quantities of GF on the mechanical and thermal characteristics, thermal stability, and flame resistance of the composite samples. Additionally, the feasibility of using GF/bio-derived PBz composites for dental posts was analyzed through finite element analysis (FEA). The stress distribution in a tooth model repaired with the newly developed GF/bio-derived PBz composite posts under oblique loads was compared to models repaired with conventional glass fiber post and gold alloy post. The incorporation of GFs significantly enhanced the flexural properties, thermal stability, and flame resistance of the composite samples, while also reducing thermal expansion in a manner that closely matched that of dentin. The FEA of a tooth model repaired with a composite post derived from GF/bio-based PBz revealed a stress distribution pattern comparable to that of a tooth model repaired using a conventional glass fiber post. Considering the composite's mechanical properties, thermal stability, flame resistance, and its suitability for dental fiber posts as demonstrated by the FEA, the GF/bio-derived PBz holds significant promise for use in dental fiber post applications.

Keywords: dental composites; eco-friendly materials; phenolics; E-glass fibers; infrared spectroscopy; innovation



Academic Editor: Danijela Marović

Received: 30 January 2025

Revised: 7 March 2025

Accepted: 7 March 2025

Published: 9 March 2025

Citation: Mora, P.; Rimdusit, S.; Jubsilp, C. Characteristic Evaluation and Finite Element Analysis of a New Glass Fiber Post Based on Bio-Derived Polybenzoxazine. *Int. J. Mol. Sci.* **2025**, *26*, 2444. <https://doi.org/10.3390/ijms26062444>

Copyright: © 2025 by the authors. Licensee MDPI, Basel, Switzerland. This article is an open access article distributed under the terms and conditions of the Creative Commons Attribution (CC BY) license (<https://creativecommons.org/licenses/by/4.0/>).

1. Introduction

Numerous advancements in material performance over the past decade can be credited to the evolution of multicomponent polymer systems, particularly through the use of multiphase materials like fiber and filler reinforcement in polymer matrix composites [1–8]. In recent times, thermosetting polymers have garnered significant interest from the automotive, aerospace, and construction sectors due to their substantial potential. Polybenzoxazines represent a novel category of phenolic polymers designed as an alternative to conventional high-performance thermosetting polymers, offering a diverse array of desirable attributes while addressing various limitations of traditional novolac and resole-type phenolic resins. They exhibit remarkable characteristics, including excellent stiffness, a relatively high glass transition temperature despite having a low cross-linking density, high char yield, and minimal water absorption. They can also be customized to achieve various properties, spanning from advanced epoxies and phenolic resins to bismaleimides and polyimides. In addition, their monomers, benzoxazines, demonstrate a low a-stage viscosity, facilitating formulation with a wide variety of fibers, minimal volumetric change

during polymerization, they do not necessitate strong acid catalysts, and they do not generate any toxic by-products [9,10]. Due to the exceptional characteristics of polybenzoxazine, they are consistently employed as polymer matrices in fiber-reinforced composites that possess significant potential for use as heat-resistant, insulating, and structural materials, thanks to their outstanding thermal, mechanical, and electrical characteristics. Each polybenzoxazine/fiber composite exhibits unique properties that require appropriate processing techniques [11–14]. A thorough assessment has been conducted of the mechanical, thermal, and electrical attributes of these composites. Okhawilai et al. [15] examined the impact performance of the composite from glass and aramid fiber-reinforced polybenzoxazine/polyurethane composites. Their findings revealed that, with an equal number of plies, the deformation in the final panel of the S-glass composite was notably less than that of the E-glass composite specimen. These panels were evaluated for their resistance, and all specimens successfully withstood projectile penetration. The results obtained from this study demonstrate that these panels possess exceptional ballistic properties, making them suitable raw materials for body armor manufacturing. Advanced composite materials with mechanical integrity and self-extinguishing properties were presented by Jubsilp et al. [16]. They evaluated mechanical carbon fiber (CF) composites using polybenzoxazine modified with pyromellitic dianhydride as a matrix. The flexural modulus and strength of the composites were increased with an increase in CF content up to 65 wt% (57 vol%). The obtained flexural properties of the composite were still higher than those of carbon fiber-reinforced bisphenol-A-based epoxy composites. In addition, the carbon fiber composites also achieved the maximum V-0 fire-resistant classification. Wolter et al. [2] discovered that GF-reinforced polybenzoxazine composites exhibited commendable fire, smoke, and toxicity (FST) properties, comparable to or even superior to GF-reinforced epoxies in railway applications. Consequently, the developed composite has the potential to maintain elevated fire safety standards in industries such as railways, eliminating the need for additional flame-retardant additives. A fiber post composed of GF-reinforced petroleum-based polybenzoxazine was developed by Mora et al. [17,18]. The composites were found to be biocompatible materials as their cell viability was found to be more than 90%. Finite element analysis was also performed to investigate the complex mechanical reactions of the glass fiber-reinforced polybenzoxazine composites under external loads. This approach is recognized for its modern technological benefits, facilitating the modeling process to be straightforward, convenient, and fast. However, the escalating global fossil fuel crisis, along with ongoing health and environmental concerns, presents significant challenges for polybenzoxazines regarding their availability and pricing. Additionally, petroleum does not readily provide a diverse range of chemical structures or functional properties. Recent research initiatives have concentrated on creating renewable substitutes to replace the phenol and amine monomers found in benzoxazines. Bio-based phenols, including eugenol [19–21], vanillin [22–26], and cardanol [27–30], have been utilized as raw materials in the production of bio-based polybenzoxazines, whereas for bio-based amines, furfurylamine and stearylamine are the preferred choices [31–33]. The aim is to create a green process that transforms these raw materials into final products, with the goal of developing a bio-based and biodegradable polybenzoxazine that aligns with the principles of green chemistry [10].

In recent years, research has focused on the use of bio-based polybenzoxazine as a matrix for fiber-reinforced composites, exploring its potential applications in various fields such as coatings, construction, and the transportation industry, including automotive and aerospace interior panels. Using glass fiber-reinforced eugenol/furfurylamine-derived benzoxazine/epoxidized castor oil (E-fa/ECO) copolymers activated by near-infrared light, a new sustainable self-healing polymer composite was created [3]. The thermal properties

and stability of the sustainable composites showed significant improvements with the addition of reinforcing glass fiber, and the flexural strength of the composites was also enhanced by incorporating GF, reaching levels of up to 70 wt%. In addition, the composites demonstrated effective macroscopic thermal healing capabilities, achieving results between 64% and 86%, suggesting their possible application as building lath. Luengrojanakul et al. [22] studied the effects of adding CF and graphene nanoparticles (GnPs) on the mechanical and shape memory properties of vanillin/furfurylamine-based polybenzoxazine (V-fa)/ECO composite. The results demonstrated that adding GnPs and CF enhanced both the flexural strength and modulus due to improved interfacial adhesion and fiber reinforcement, with the best results seen at 3 wt% GnPs and 60 wt% CF. Furthermore, the optimal compositions for achieving the best performance of the bio-based SMP composite were found to be 40 wt% CF and 3 wt% GnPs. The eugenol/furfurylamine-derived polybenzoxazine (E-fa) and eugenol/stearylamine-derived polybenzoxazine (E-sa) and jute fiber (a bio-fiber) were used to prepare bio-based polybenzoxazine/jute fiber composites [21]. It was found that the modulus and glass transition temperature of the E-fa and E-sa were enhanced with the addition of jute fiber. Previous research indicates that reinforcing bio-based polybenzoxazine with glass fiber (GF) enhances its mechanical and thermal properties sufficiently to meet the necessary characteristics for fiber post materials. This includes physical properties like the modulus of elasticity, flexural strength, and thermal expansion, which closely resemble those of dentin. Furthermore, the use of bio-based polybenzoxazine as a substitute for epoxy resins—commonly used as the polymer matrix for glass fiber posts—offers a solution to the drawbacks associated with epoxy resins, such as the use of toxic hardeners and potential irritation to the eyes and skin from prolonged exposure. In addition, it is anticipated that the benefits of glass fiber-reinforced bio-based polybenzoxazine posts will be realized in several areas, including their ease of handling, mechanical properties, esthetic appeal, removability, and their potential as biocompatible materials.

Therefore, in this work, a new polymer composite post has been developed utilizing a vanillin/furfurylamine-based polybenzoxazine, reinforced with GF. The effect of GF content on the mechanical and thermal characteristics, thermal stability, and flame resistance was evaluated. In addition, the mechanical response to externally applied loads of the composite post, utilizing FEA, was assessed. The findings from the simulations will be contrasted against data from commercially available GF post and gold alloy post.

2. Results and Discussion

2.1. Characteristics of V-Fa and Poly(V-Fa)

FT-IR spectroscopy was used to examine the structure of the synthesized V-fa. The V-fa spectrum is shown in Figure 1a. Distinct absorption peaks associated with furan rings are identified at 1580 and 760 cm^{-1} . The peak observed at 1685 cm^{-1} confirms the existence of the formyl group in vanillin. Additionally, the absorption peak at 1021 cm^{-1} , which corresponds to the asymmetric stretching of C-N-C, and at 1229 cm^{-1} , indicative of the Ar-C-O stretch, suggests that an oxazine ring is integrated with vanillin's benzene ring [23,34]. In addition, the weak bands observed at 3025 and 2924 cm^{-1} are attributed to the asymmetric and symmetric stretching of the aromatic -CH group, respectively. These findings thereby validate the formation of V-fa, as shown in Figure 1b.

The curing characteristics of V-fa were examined using differential scanning calorimetry (DSC). The DSC thermogram for V-fa is depicted in Figure 1c. It was found that the endothermic peak at 120 °C indicates the melting temperature (T_m) of V-fa, while the exothermic trend sheds light on the curing process. The curing begins at an onset temperature (T_{onset}) of 160 °C, reaches its maximum curing temperature (T_{max}) at 200 °C, and completes at the final curing temperature (T_{final}) of 230 °C. This indicates that achieving

a temperature of 250 °C is essential for the full polymerization of V-fa. Additionally, the total heat released during the curing/polymerization process is calculated to be 125 J/g. Thus, the curing behavior of V-fa occurs at a temperature that is 30 °C lower than the conventional petroleum-based benzoxazine, specifically the bisphenol-A/aniline-based benzoxazine (BA-a), which has a T_{\max} of 230 °C [35]. This reduction in curing temperature suggests that the formyl group present in vanillin plays a significant role, as it has been previously noted that it can easily oxidize to a carboxylic group, which facilitates the ring-opening polymerization of V-fa [36,37]. Following the curing process, polymerized V-fa was obtained, as evidenced in Figure 1a, which displays a broad peak around 3100–3800 cm^{-1} and a distinctive band at 3350 cm^{-1} corresponding to the hydroxyl group produced by the thermal ring-opening reaction of the oxazine ring. The proposed curing reaction of the V-fa is also exhibited in Figure 1b.

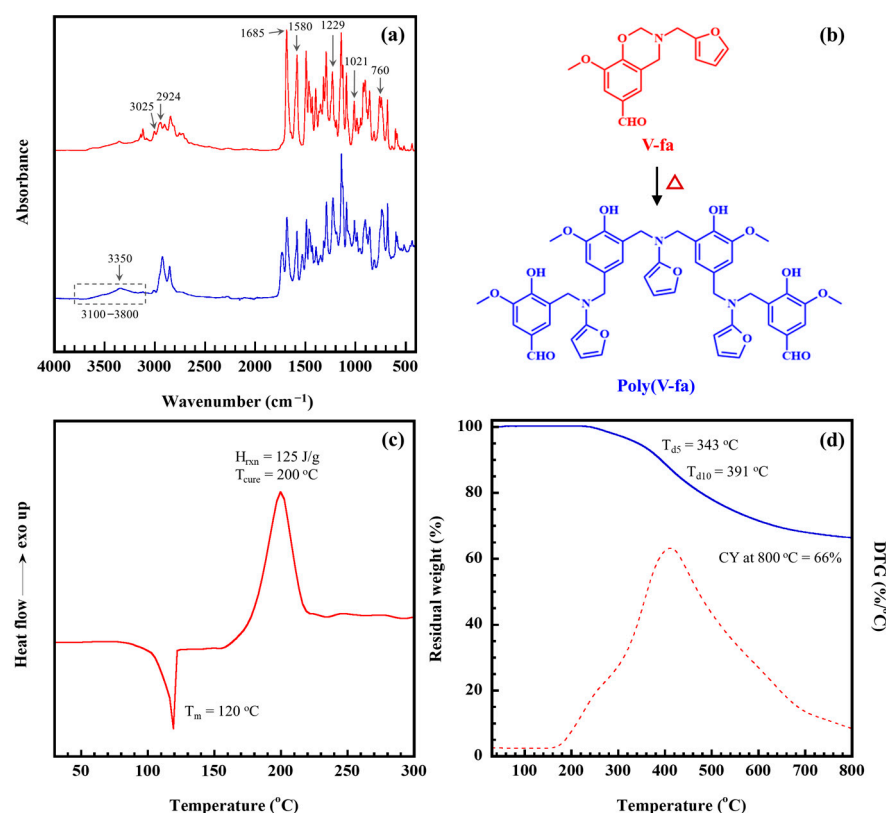


Figure 1. Characteristics of V-fa and poly(V-fa): (a) FT-IR spectrum of V-fa, (b) Structure of the synthesized V-fa, (c) DSC thermogram of V-fa, (d) TGA thermogram of poly(V-fa).

The thermal stability of poly(V-fa) was evaluated through thermogravimetric analysis (TGA), as shown in Figure 1d. This figure illustrates the weight loss of poly(V-fa) in correlation with temperature and includes its derivative thermogravimetric curve (DTG). The thermogram indicates that degradation occurs in two steps, with poly(V-fa) maintaining thermal stability up to 230 °C. The first step of the degradation of poly(V-fa) transpires between 200 and 300, while the second step transpires between 300 and 700 °C. The temperature at which 5% degradation (T_{d5}) is observed is 343 °C, while 10% degradation (T_{d10}) is detected at 391 °C. These observations suggest that the degradation temperature of poly(V-fa) closely resembles that of bisphenol-A/aniline PBz, i.e., $T_{d5} \sim 337\text{ °C}$ [38]. Additionally, a char yield of 66% was achieved after heating to 800 °C, demonstrating a higher char yield compared to conventional dibenzene-based polybenzoxazines, such as those derived from bisphenol-A, which typically show a char yield between 28% and 32% at 800 °C [9].

This suggests that the network incorporating furan significantly enhances char formation in polybenzoxazines.

2.2. Flexural Properties of GF/Poly (V-Fa) Composites

As seen in Figure 2a, the effect of GF content on the flexural characteristics of poly(V-fa) composites was investigated. As more glass fiber was added—between 33.0 and 42.5 vol%—the strength of the composites rose significantly, from 323.2 ± 16.2 to 460.4 ± 20.4 MPa, respectively. This increase in flexural strength can be attributed to a robust interfacial bond between the glass fiber and the polymer matrix [17,18,34]. However, with an increase to 66.3 vol% glass fiber content, the strength slightly declined to 429.5 ± 7.7 MPa. The slight decline in strength is probably attributed to the reduced content of the poly(V-fa) matrix. This reduction affects the GF/poly(V-fa) interface, which is a crucial factor impacting on the overall macroscopic properties of the composite, including its strength, as it leads to diminished stress transfer between the GF and poly(V-fa). The results suggested that the reinforcement of GF at 53.5 vol% into poly(V-fa) showed high flexural strength for further dental post material applications. Furthermore, the flexural modulus of the composites was found to improve with higher GF content, exhibiting values that ranged from 9.8 ± 0.5 to 25.6 ± 1.52 GPa. The necessary elastic modulus, which is a crucial factor for load transmission, should therefore be close to that of dentin, i.e., 18 to 40 GPa [39–42], in order to use the glass fiber-reinforced poly (V-fa) composite as a glass fiber post. Since the experimental density of the GF/poly(V-fa) composites followed the rule of mixture, as shown in Figure 2b, the enhancement of the composites' flexural properties with rising GF content aligned with their experimental density.

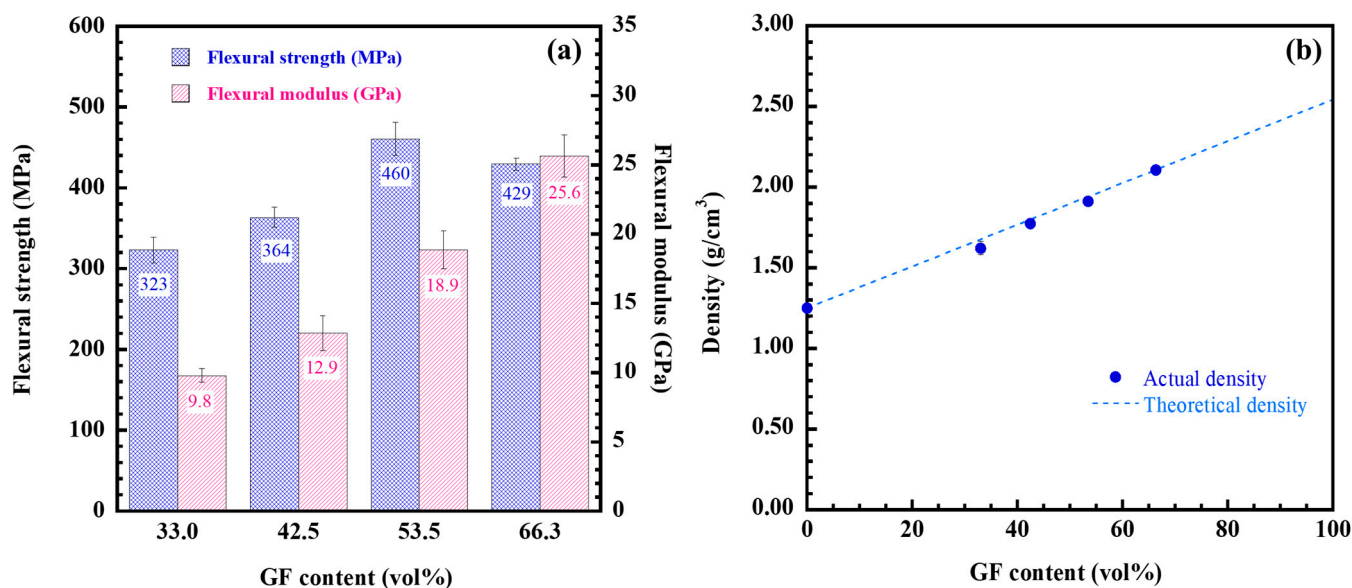


Figure 2. (a) Flexural property of poly(V-fa) composites at various GF contents, (b) Density of GF-reinforced poly(V-fa) composites at various GF contents: (●) Actual density, (---) Theoretical density.

2.3. Thermal Expansion of GF/Poly(V-Fa) Composites

The coefficient of thermal expansion (CTE) of restorative materials for dental restoration was analyzed due to their expansion upon heating from hot foods and beverages, along with contraction when exposed to cold. This disparity in CTE between the dental tissue and the restorative materials can lead to fractures during the cycles of expansion and contraction. To explore their potential use as new dental fiber posts, the CTE values of GF/poly(V-fa) composites were evaluated. Figure 3a depicts the displacement of the composite samples ranging from 33.0 to 66.3 vol% GF over a temperature range of 20

to 150 °C. All of the tested composites exhibited greater displacement with increasing temperature; however, at a specific temperature, higher GF loadings resulted in reduced displacement of the samples.

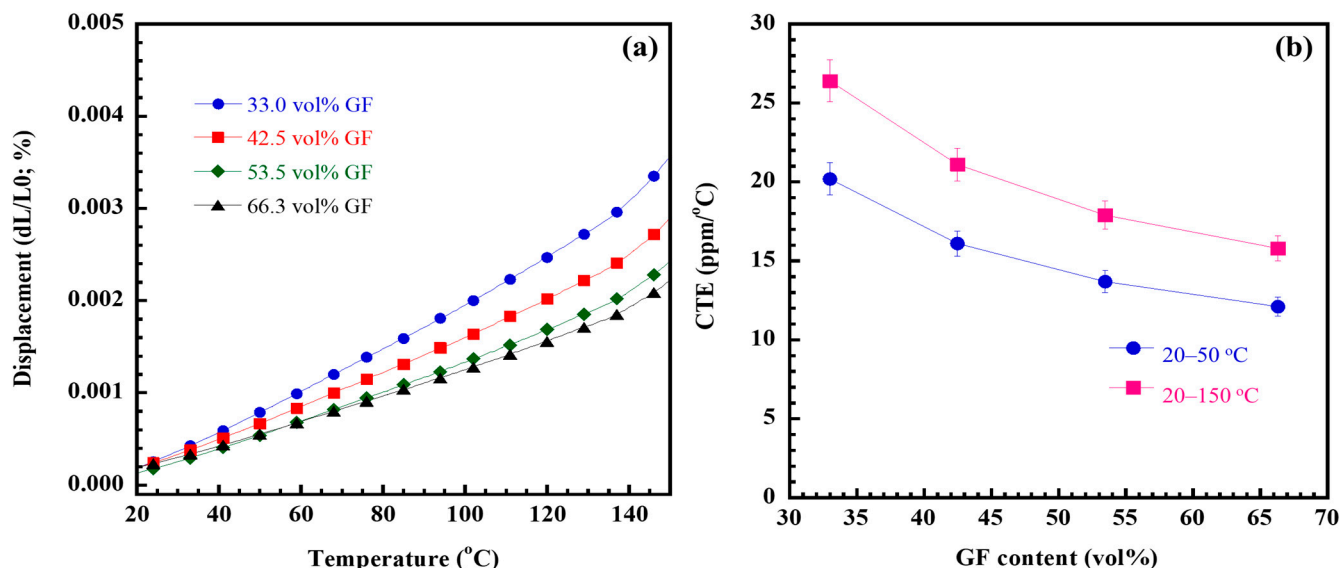


Figure 3. (a) TMA curves of GF/poly(V-fa) composites at various GF contents; (b) CTE of the composites in the glassy region from 20 to 50 °C and from 20 to 150 °C.

Figure 3b presents the average CTE values for the glassy state of the GF/poly(V-fa) composite samples, as derived from the slopes in Figure 3a for the temperature ranges of 20 to 50 °C and 20 to 150 °C. The CTE for the composite samples over the 20–150 °C interval was observed to reduce their CTE values with an increase in GF content. Specifically, the CTE values dropped to 26.4, 21.1, 17.9, and 15.8 ppm/°C for composites containing 33.0, 42.5, 53.5, and 66.3 vol% GF, respectively. Likewise, during the 20–50 °C range, the CTE of the composite samples also showed a decline with rising GF content from 33.0 vol% to 66.3 vol%, recording values of 20.2, 16.1, 13.7, and 12.1 ppm/°C, respectively. The decreased CTE values of the composite samples can be attributed to the inherently lower CTE value of GF compared to the polymer matrix, specifically ranging from 5 to 12 ppm/°C. Additionally, the higher rigidity of the GF, with a modulus of 70 to 85 GPa, contributes to the limited motion of the macromolecular segments in poly(V-fa). Furthermore, the interfacial adhesion between the GF and the poly(V-fa) matrix significantly influences the reduction in the CTE of the composites. In comparison with GF/poly(BA-a) composites [17], the GF/poly(V-fa) composites showed high performance with lower CTE values than that of GF/poly(BA-a) composites, which would cause lower thermal stress and high dimensional stability.

In order to utilize GF/poly(V-fa) composites as dental glass fiber posts in tooth restoration, it is crucial to compare their CTE values with those of dental tissues, like dentin, rather than evaluating the CTE of each material individually. The analysis indicated that the CTE of the composite containing 33.0 vol% and 66.3 vol% was approaching that of dentin, which is approximately 11 ppm/°C at temperatures between 10 and 80 °C [43], typical for tooth exposure during the consumption of hot beverages and food. As a result, the CTE for poly(V-fa) composite with the 53.5 vol% and 66.3 vol% closely matches that of dentin, which helps minimize stress buildup at the dentin–post interface and effectively prevents the loss of marginal adaptation.

2.4. Thermomechanical Properties of GF/Poly(V-Fa) Composites

Using dynamic mechanical analysis (DMA), the viscoelastic characteristics of the GF/poly(V-fa) composites with different GF contents were investigated. Table 1 lists key DMA metrics for the composite samples, including the temperature-dependent damping factor ($\tan \delta$), loss modulus (E''), and storage modulus (E'). The E' values in the glassy state of the composite samples, known as the dynamic modulus, indicate the material's stiffness and elastic behavior, and they showed an upward trend with higher GF contents. These findings align well with the flexural properties discussed earlier. On the other hand, the glass transition temperature (T_g) is determined as the localized maximum in the loss modulus, which is a crucial factor concerning molecular mobility. As the composite samples approach and surpass the peak, the dissipated energy rises due to the relatively extensive segmental movement of the poly(V-fa).

Table 1. Thermomechanical properties of GF/poly(V-fa) composites.

Composite Samples	E' (GPa)	T_g from E''
33.0 vol% GF/poly(V-fa)	12.5	164
42.5 vol% GF/poly(V-fa)	15.4	167
53.5 vol% GF/poly(V-fa)	18.0	170
66.3 vol% GF/poly(V-fa)	19.8	170

From Table 1, it can be seen that the amount of GF in the GF/poly(V-fa) composite samples increased, and the T_g of the composite samples also rose. Specifically, the T_g values for the composite samples, deduced from E'' , were noted to range from 164 to 170 °C. This increase in T_g can be linked to the GF's capacity to enhance interfacial adhesion within the composite, which in turn supports the movement of poly(V-fa) molecular chains, much like what has been studied in GF/poly(BA-a) composites [18] and GF/poly(E-fa) composites [44]. The working temperature of dental materials in contact with human teeth exposed to hot foods and drinks was found to be around 36 °C to 48 °C [45], and the actual intraoral temperature varies between approximately 5 °C and 55 °C [43]. Consequently, it was noted that the glass transition temperature (T_g) of the GF/poly(V-fa) composite samples exceeded the temperature range of 5–55 °C, suggesting that the composites exhibit strong mechanical properties at working temperatures.

2.5. Thermal Stability of GF/Poly(V-Fa) Composites

The thermal degradation of fiber-reinforced polymer composites plays a vital role in structural applications by offering valuable information about material performance, load-bearing capacity at specific temperatures, and dimensional stability when exposed to high temperatures. As a result, assessing the thermal stability of restorative materials is essential for determining their capability to endure the elevated temperatures generated during tooth restoration without undergoing decomposition. To evaluate the thermal stability of the GF/poly(V-fa) composites, the TGA thermogram of poly(V-fa) composites containing varying amounts of GF is shown in Figure 4a, while the data on thermal degradation at 5% weight loss (T_{d5}) and residual weight or char yield (CY) at 800 °C for the poly(V-fa) composites are illustrated in Figure 4b.

It was noted that as the GF content in the poly(V-fa) composites increased, the T_{d5} also rose. This indicates that the incorporation of GF enhances the thermal stability of the poly(V-fa) composites, as the degradation temperature of GF exceeds 800 °C [46]. This reinforcement prevents the direct thermal degradation of poly(V-fa) by providing a shielding effect against heat. Additionally, GF plays a role in impeding the release of volatile organic compounds during the thermal breakdown of poly(V-fa). When evaluating

the working temperature of dental materials in relation to human teeth exposed to hot foods and beverages (approximately 36 to 48 °C), as well as the maximum oral temperatures recorded around the front teeth due to hot liquids (around 70 °C), it was found that the degradation temperature of poly(V-fa/ECO) composites across all ratios of GF reinforcement was higher.

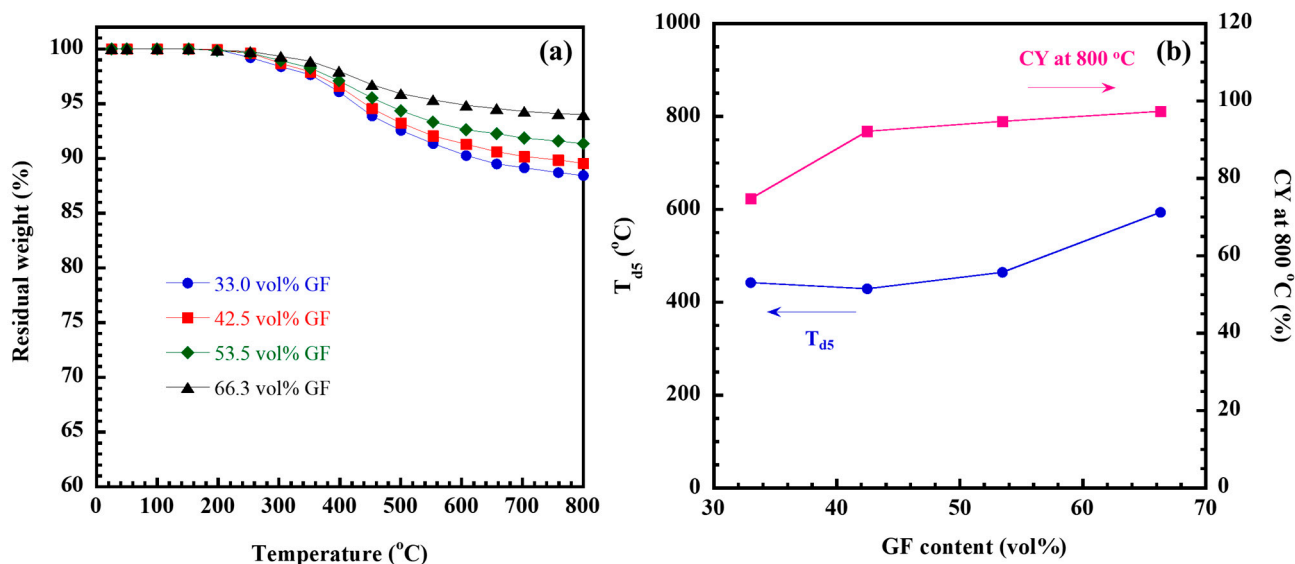


Figure 4. (a) TGA thermograms and (b) T_{d5} and CY at 800 °C of GF/poly(V-fa) composites at various GF contents (vol%).

Furthermore, the CY of the poly(V-fa) composites at 800 °C in nitrogen atmosphere, as depicted in Figure 4b, also showed an increase from 74.7% to 97.3% with the addition of GF from 33.0 vol% to 66.3 vol%. This property arises from the mineral composition of GF, which is inherently non-combustible and does not release any toxic substances when subjected to heat. Consequently, the high char yield obtained indicates that the GF/poly(V-fa) exhibits outstanding thermal stability and is likely to demonstrate effective flame retardancy.

To assess the flame-retardant properties of the GF/poly(V-fa) composites, the limiting oxygen index (LOI) serves as a key measurement. It can be determined by using the CY obtained during pyrolysis in nitrogen atmosphere combined with the Van Krevelen and Hoftzyer equation (Equation (1)).

$$LOI = 17.5 + 0.4CY \quad (1)$$

As a result, the poly(V-fa) composites reinforced with glass fiber exhibit a char yield ranging from 74.7 to 97.3, resulting in LOI values between 47.4 and 56.4. These parameters indicate that the composites demonstrate self-extinguishing characteristics.

2.6. Feasibility of GF/Poly(V-Fa) Composites for Dental Fiber Post by FEA

Figure 5 shows the von Mises stress (σ_v) distribution in the root dentin structure and the post for the GF/poly(V-fa) composite posts with various GF contents. The magnitude of the maximum σ_v in the tooth structures and in the post was also recorded. It can be seen that the maximum σ_v presented at the dentin region and cervical thirds of the root and reduced from 20.900 to 20.885 MPa for the composite samples reinforced with GF of 33.0–66.3 vol%, respectively. The reduction in maximum σ_v in the dentin region caused by the composite post reinforced with a higher GF contents could be carried by the larger load fraction, i.e., 2.2069, 2.548, 3.4863, and 4.3082 MPa. This behavior was similar to the tooth

restored with GF post based on bisphenol-A/aniline polybenzoxazine [18]. GF/poly(V-fa) composite at 53.5 vol% GF may be the material for a post application given its dentin-like elastic modulus and lower stress generation in the remaining dentin.

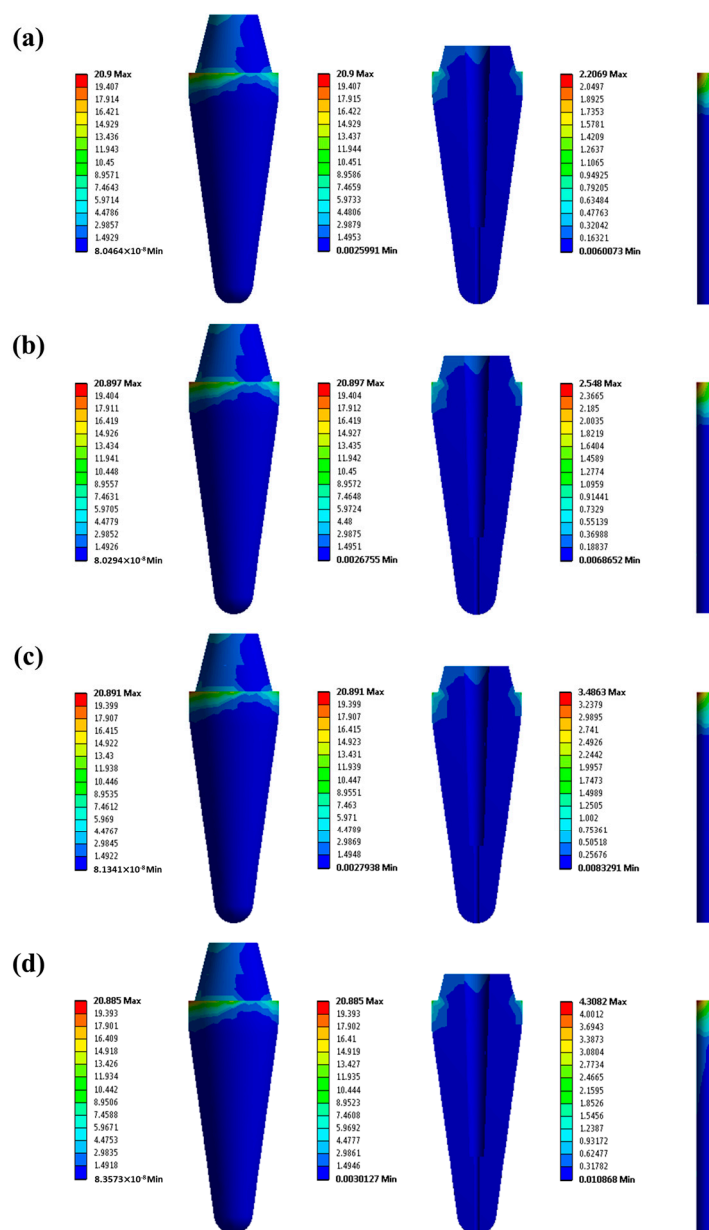


Figure 5. σ_v distribution of tooth restored with GF/poly(V-fa) composite post at various GF contents: (a) 33.0 vol%, (b) 42.5 vol%, (c) 53.5 vol%, and (d) 66.3 vol%.

To evaluate the performance of the developed 53.5 vol% GF/poly(V-fa) composite post in comparison to commercial GF and gold alloy posts, the σ_v distribution on a restored tooth model was assessed and is presented in Figure 6. It was observed that all the models showed the highest σ_v in the cervical region of the dentin. Notably, the model restored with the composite post displayed a maximum σ_v value of 28.267 MPa, which was similar to 28.320 MPa for the model using the commercial GF post. The model restored with gold alloy post showed the lower maximum σ_v , i.e., 20.799 MPa, than the model restored with GF posts. The results indicate that the GF/poly(V-fa) composite post can support a greater load fraction due to its elastic modulus being comparable to that of dentin. Furthermore, compared to restorations using gold alloy posts, the minimal color change seen at the apical

third of the root indicates effective occlusal load dissipation, greatly lowering the risk of vertical fractures.

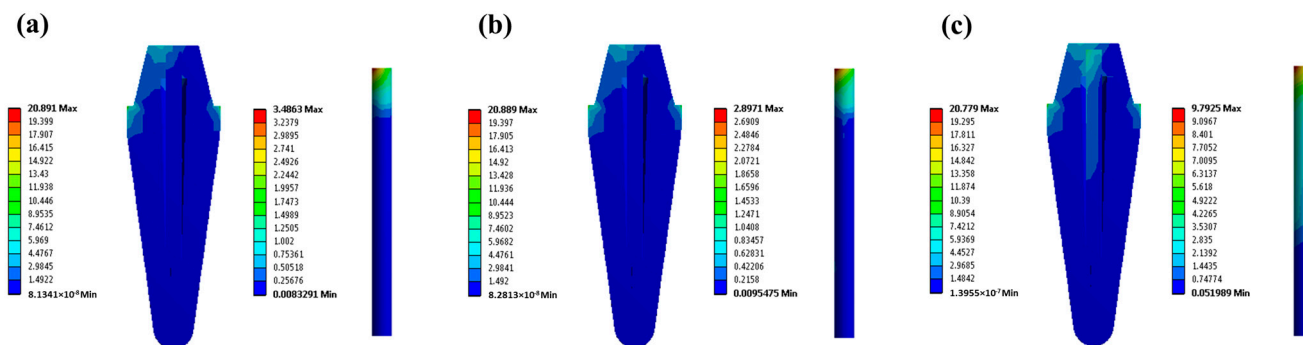


Figure 6. σ_v distribution of tooth restored with posts: (a) 53.5 vol% GF/poly(V-fa) composite post, (b) commercial GF post, and (c) gold alloy post.

3. Materials and Methods

3.1. Materials

Vanillin (99%) and furfurylamine (>99%) were sourced from Sigma-Aldrich Pte. Ltd. in Singapore, while paraformaldehyde (AR grade) was obtained from Merck Co., Ltd. based in Darmstadt, Germany. All chemicals were utilized in their received state. Additionally, plain weave glass fiber (GF) fabrics with an areal density of 600 g/m² were acquired from Thai Polyadd Ltd. Partnership (Bangkok, Thailand).

3.2. Benzoxazine Resin, Prepreg, and Composite Preparation

The bio-derived benzoxazine resin (V-fa) was synthesized through a solvent-free process utilizing biobased raw materials, vanillin, furfurylamine, and paraformaldehyde, in a molar ratio of 1:2:1. The reaction generated a dark brown liquid resin, achieved by continuously mixing the three ingredients for 40 min at 110 °C. The GF/poly(V-fa) composites using different GF contents of vol% were prepared as illustrated in Figure 7. The molten V-fa resin was then pre-impregnated onto GF at a temperature of 80 °C. Subsequently, the composite laminates underwent a preheating process at temperatures ranging from 150 to 170 °C for 3 h, before being cured at 180 °C for 2 h under a pressure of 15 MPa in a compression mold. The cured V-fa was characterized after cooling down to room temperature. The differential scanning calorimetry (DSC) technique indicated a complete curing conversion of 100% for the GF/poly(V-fa) composites, demonstrating that the composites were fully cured.

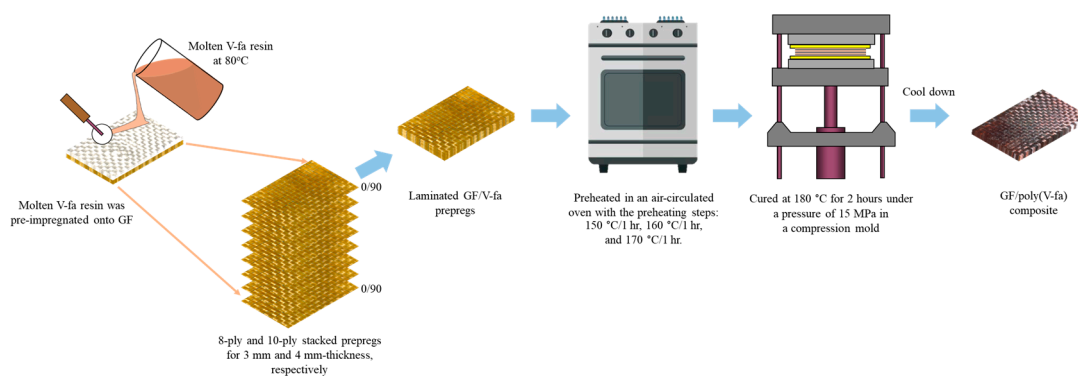


Figure 7. Preparation of GF/poly(V-fa) composites.

The GF volume percentage in the poly(V-fa) composites (V_f) can be calculated through Equation (2):

$$V_f = \frac{W_f / \rho_f}{W_f / \rho_f + W_m / \rho_m} \quad (2)$$

where W_f is the weight of GF, W_m is the weight of poly(V-fa), ρ_f is the density of GF, and ρ_m is the density of poly(V-fa). The ρ_f and ρ_m are 2.54 and 1.25 g/cm³, respectively.

3.3. Samples Characterization

The composite density is assessed through the water displacement method, following the guidelines set by ASTM D792-20 [47]. The three samples were tested, and their average density values were reported.

A differential scanning calorimeter, DSC1 Module from Mettler Toledo Ltd. (Bangkok, Thailand), was employed to measure the melting temperature (T_m) and curing characteristics of V-fa. Using a sample weight of 5 mg contained in an aluminum pan, the experiments were carried out in a N₂ environment at a heating rate of 10 °C/min.

The Universal Testing Machine was used to analyze the composite's flexural properties in compliance with ASTM D790M-93 [48]. The specimens' measurements were 60 mm × 25 mm × 3 mm. A three-point bending test with a 48 mm support span and a crosshead speed of 1.2 mm/min was performed. The support span-to-thickness of the sample's ratio is 16:1. Five samples of each composite composition were tested, and the average values were reported.

The dynamic viscoelastic analyzer (model DMA1, Mettler Toledo) was used to assess the samples' dynamic mechanical characteristics. Throughout the process, a three-point bending test was used. At a frequency of 1 Hz and an amplitude of 30 µm, strain was measured. The samples, which had dimensions of 10 mm × 50 mm × 3 mm, were heated from 30 to 300 °C at a rate of 2 °C/min.

The Mettler Toledo thermogravimetric analyzer (model TGA1 Module) was used to evaluate the samples' thermal stability. During the analysis, the specimens were heated from 25 to 800 °C at a rate of 20 °C/min while being continuously supplied with 50 mL/min of N₂.

A thermomechanical analyzer (TMA) (Bruker-AXS, TMA 4010, Bangkok, Thailand) was employed to determine the CTE of the samples. The specimens, measuring 10 mm × 5 mm × 4 mm, were examined at an average heating rate of 5 °C/min within the temperature range of 100–200 °C, applying a constant load of 5 mN (0.5 g) in a nitrogen environment. The CTE for each sample was obtained by averaging three measurements.

3.4. Finite Element Analysis (FEA)

ANSYS Inc., in Canonsburg, Pennsylvania-based company, used the Design Modeler feature in ANSYS Workbench 2022 R1 (file version 22.1.0.2021111419) software to create the 3D model. The GF/poly(V-fa) composite post, gutta-percha, composite resin, dentin, crown, periodontal ligament, cortical bone, cancellous bone, and gingiva are all included in the model of the endodontically treated tooth, as shown in Figure 8a. The analysis of the 3D finite element method (FEM) was conducted using ANSYS Workbench 2022 R1 software. Subsequently, a 3D mesh was developed consisting of solid elements characterized by nodes. For the tooth restored with post models, there were 7074 elements and 13,195 nodes created (Figure 8b). A 100 N axial load was applied obliquely from the buccal to the lingual region at a 45° angle to the tip of the buccal cusp (Figure 8c). The outer surface of the bone could not move freely in any of the models.

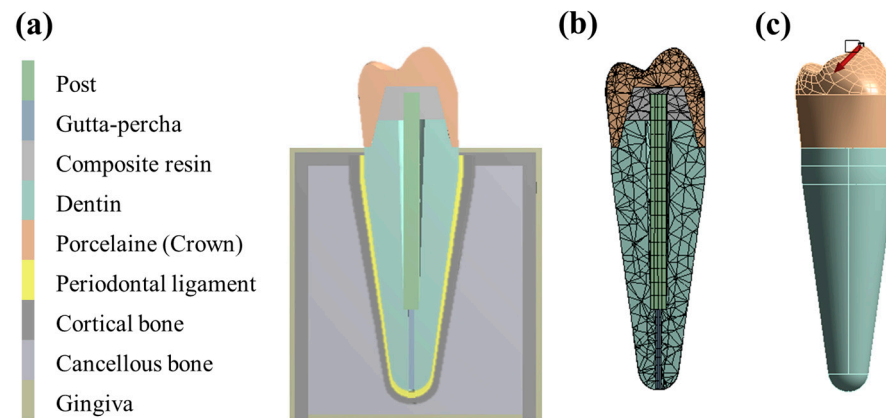


Figure 8. (a) Tooth model repaired with GF/poly(V-fa) composite, commercial GF, and gold alloy posts, (b) 3D mesh of tooth model, and (c) 100 N oblique load at 45° angle.

Table 2 lists all of the materials and structures that were categorized as isotropic, homogeneous, and linearly elastic. These included gutta-percha, composite resin, dentin, crown, periodontal ligament, cortical bone, cancellous bone, gingiva, and gold alloy. On the other hand, GF/poly(V-fa) composites, which are used as glass fiber posts, are classified as orthotropic materials, which means that their properties vary along three orthogonal axes, as Table 3 illustrates.

Table 2. Elastic characteristics of the isotropic materials input into this study [17,37,49].

Material	Elastic Modulus	Poisson's Coefficient
Gutta-percha	6.9×10^{-4}	0.45
Composite resin	16.6	0.24
Dentin	18.6	0.31
Porcelain (crown)	120	0.28
Periodontal ligament	6.89×10^{-2}	0.45
Cortical bone	13.7	0.30
Cancellous bone	1.37	0.30
Gingiva	19.6×10^{-3}	0.30
Gold alloy	93.0	0.33

Table 3. Elastic characteristics of the orthotropic materials input into this study.

Elastic Constant	GF/Poly(V-Fa) Composite Post at Various GF Contents (vol% (wt%))				Commercial GF Post [49]
	33.0 (50)	42.5 (60)	53.5 (70)	66.3 (80)	
E_L , GPa	9.80	12.90	18.90	25.60	37.0
$E_T = E_{T'}$, GPa	6.39	7.92	10.31	14.59	9.50
$G_{LT} = G_{LT'}$, GPa	3.58	4.32	5.47	7.50	3.10
$G_{TT'}$, GPa	2.44	3.05	4.03	5.82	3.50
$\nu_{LT} = \nu_{LT'}$	0.25	0.24	0.23	0.22	0.27
$\nu_{TL} = \nu_{T'L}$	0.17	0.15	0.13	0.12	0.27
$\nu_{TT'}$	0.31	0.30	0.28	0.25	0.34

Note: E_L obtained from experimental data, as reported in item 2.2, while the other elastic properties were calculated theoretically using the equations presented by Pegoretti et al. [49]. The elastic moduli for poly(V-fa) and glass fiber are 3.09 GPa and 72 GPa, respectively.

4. Conclusions

GF-reinforced composites made from bio-derived polybenzoxazine, which is synthesized from vanillin and furfurylamine, were successfully developed. The addition of GF positively affected the mechanical and thermal properties, with notable improvements in flexural modulus and strength, glass transition temperature, degradation temperature, and flame resistance observed as the GF content increased. Furthermore, GF reinforcement significantly reduced the CTE due to the robust structural integrity of GF within the bio-derived polybenzoxazine matrix. All composite samples exhibited LOI values significantly surpassing the threshold for self-extinguishing materials. The GF-reinforced bio-derived polybenzoxazine post exhibits an elastic modulus that aligns more closely with that of dentin, in contrast to the significantly higher modulus of a conventional glass fiber post and gold alloy post. Therefore, this study suggests that GF-reinforced bio-derived polybenzoxazine could be an excellent choice for post applications that demand both strong mechanical and thermal properties, and environmentally friendly materials.

Author Contributions: Conceptualization, C.J.; methodology, P.M.; formal analysis, C.J. and P.M.; writing—original draft preparation, P.M.; writing—review and editing, C.J. and S.R.; visualization, C.J. and P.M.; supervision, C.J.; project administration, C.J.; funding acquisition, C.J. and S.R. All authors have read and agreed to the published version of the manuscript.

Funding: This research was funded by Fundamental Fund 2022, Thailand Science Research and Innovation (TSRI) via Srinakharinwirot University, grant number 042/2565, the National Research Council of Thailand (NRCT) and Srinakharinwirot University, grant number N42A650377, Srinakharinwirot University Development, grant number 588/2565, and the National Research Council of Thailand (NRCT) and Chulalongkorn University, grant number N42A660910.

Institutional Review Board Statement: Not applicable.

Informed Consent Statement: Not applicable.

Data Availability Statement: Data are contained within the article.

Acknowledgments: All contributors who assisted in this research are acknowledged in the Author Contributions list.

Conflicts of Interest: The authors declare no conflicts of interest.

References

- Magalhães, N.; Maia, B.A.; Braga, M.H.; Santos, R.M.; Correia, N.; Cunha, E. Glass fiber reinforced epoxy-amine thermosets and solvate IL: Towards new composite polymer electrolytes for lithium battery applications. *Int. J. Mol. Sci.* **2023**, *24*, 10703. [[CrossRef](#)] [[PubMed](#)]
- Wolter, N.; Beber, V.C.; Sandinge, A.; Blomqvist, P.; Goethals, F.; Hove, M.V.; Jubete, E.; Mayer, B.; Koschek, K. Carbon, glass and basalt fiber reinforced polybenzoxazine: The effects of fiber reinforcement on mechanical, fire, smoke and toxicity properties. *Polymers* **2020**, *12*, 2379. [[CrossRef](#)] [[PubMed](#)]
- Mora, P.; Rimdusit, S.; Jubsilp, C. Near-infrared light-induced sustainable self-healing polymer composites from glass fabric reinforced benzoxazine/epoxy copolymers. *J. Mater. Res. Technol.* **2024**, *33*, 7808–7817. [[CrossRef](#)]
- Yadav, R.; Sonwal, S.; Sharma, R.P.; Saini, S.; Huh, Y.S.; Brambilla, E.; Ionescu, A.C. Ranking analysis of tribological, mechanical, and thermal properties of nano hydroxyapatite filled dental restorative composite materials using the R-method. *Polym. Adv. Technol.* **2024**, *35*, e70010. [[CrossRef](#)]
- Yadav, R.; Saini, S.; Sonwal, S.; Meena, A.; Huh, Y.S.; Brambilla, E.; Ionescu, A.C. Optimization and ranking of dental restorative composites by entropy-vikor and vikor-matlab. *Polym. Adv. Technol.* **2024**, *35*, e6526. [[CrossRef](#)]
- Marovic, D.; Bota, M.; Tarle, F.; Par, M.; Haugen, H.J.; Zheng, K.; Pavić, D.; Miloš, M.; Čižmek, L.; Babić, S.; et al. The influence of copper-doped mesoporous bioactive nanospheres on the temperature rise during polymerization, polymer cross-linking density, monomer release and embryotoxicity of dental composites. *Dent. Mater.* **2024**, *40*, 1078–1087. [[CrossRef](#)]

7. Marovic, D.; Par, M.; Tauböck, T.T.; Haugen, H.J.; Negovetic Mandic, V.; Wüthrich, D.; Burrer, P.; Zheng, K.; Attin, T.; Tarle, Z.; et al. Impact of copper-doped mesoporous bioactive glass nanospheres on the polymerisation kinetics and shrinkage stress of dental resin composites. *Int. J. Mol. Sci.* **2022**, *23*, 8195. [[CrossRef](#)] [[PubMed](#)]
8. Haugen, H.J.; Ma, Q.; Linskens, S.; Par, M.; Mandic, V.N.; Mensikova, E.; Nogueira, L.P.; Taubock, T.T.; Attin, T.; Gubler, A.; et al. 3D micro-CT and O-PTIR spectroscopy bring new understanding of the influence of filler content in dental resin composites. *Dent. Mater.* **2024**, *40*, 1881–1894. [[CrossRef](#)]
9. Ishida, H.; Agag, T. *Handbook of Benzoxazine Resins*, 1st ed.; Elsevier: Amsterdam, The Netherlands, 2011.
10. Ishida, H.; Froimowicz, P. *Advanced and Emerging Polybenzoxazine Science and Technology*, 1st ed.; Elsevier: Amsterdam, The Netherlands, 2017.
11. Gu, Y.; Ran, Q.-C. Polybenzoxazine/fiber composites. In *Handbook of Benzoxazine Resins*, 1st ed.; Elsevier: Amsterdam, The Netherlands, 2011; pp. 481–494.
12. Ares-Elejoste, P.; Seoane-Rivero, R.; Gandarias, I.; Iturmendi, A.; Gondra, K. Sustainable alternatives for the development of thermoset composites with low environmental impact. *Polymers* **2023**, *15*, 2939. [[CrossRef](#)]
13. Qiao, Z.; Wang, M.; Jiang, J.; Liu, H.; Wang, M.; Zhao, W.; Wang, Z. High-performance and degradable polybenzoxazine/VU vitrimer and its application for carbon fiber recycling. *ACS Sustain. Chem. Eng.* **2022**, *10*, 9113–9122.
14. Perrin, H.; Vaudemont, R.; Frari, D.D.; Verge, P.; Puchot, L.; Bodaghi, M. On the cyclic delamination-healing capacity of vitrimer-based composite laminates. *Compos. Part A Appl. Sci. Manuf.* **2024**, *177*, 107899. [[CrossRef](#)]
15. Okhawilai, M.; Hiziroglu, S.; Rimdusit, S. Measurement of ballistic impact performance of fiber reinforced polybenzoxazine/polyurethane composites. *Measurement* **2018**, *130*, 198–210. [[CrossRef](#)]
16. Jubsilp, C.; Panyawanitchakun, C.; Rimdusit, S. Flammability and thermomechanical properties of dianhydride-modified polybenzoxazine composites reinforced with carbon fiber. *Polym. Compos.* **2013**, *34*, 2067–2075. [[CrossRef](#)]
17. Mora, P.; Rimdusit, S.; Karagiannidis, P.; Srisorrchart, U.; Jubsilp, C. Biocompatibility, thermal and mechanical properties of glass fiber-reinforced polybenzoxazine composites as a potential new endodontic post. *Polym. Compos.* **2024**, *45*, 16205–16217. [[CrossRef](#)]
18. Mora, P.; Nunwong, C.; Sriromreun, P.; Kaewsriprom, P.; Srisorrachatr, U.; Rimdusit, S.; Jubsilp, C. High performance composites based on highly filled glass fiber-reinforced polybenzoxazine for post application. *Polymers* **2022**, *14*, 4321. [[CrossRef](#)] [[PubMed](#)]
19. Patil, D.A.; Naiker, V.E.; Phalak, G.A.; More, A.P.; Mhaske, S.T. Synthesis of benzoxazine from eugenol and its co-polymerization with a gallic acid-based epoxy resin for flame retardant application. *Polym. Bull.* **2024**, *81*, 7441–7465. [[CrossRef](#)]
20. Yao, H.; Lu, X.; Xin, Z.; Li, X.; Chen, C.; Cao, Y. Two novel eugenol-based difunctional benzoxazines: Synthesis and properties. *Colloids Surf. A Physicochem. Eng. Asp.* **2021**, *616*, 126209. [[CrossRef](#)]
21. Dogan, Y.E.; Uyar, T. Eugenol-derived bio-benzoxazine resins: Synthesis, characterization, and exceptional thermal stability. *J. Appl. Polym. Sci.* **2024**, *141*, e55496. [[CrossRef](#)]
22. Luengrojanakul, P.; Mora, P.; Bunyanuwat, K.; Jubsilp, C.; Rimdusit, S. Improvements in mechanical and shape-memory properties of bio-based composite: Effects of adding carbon fiber and graphene nanoparticles. *Polymers* **2023**, *15*, 4513. [[CrossRef](#)]
23. Gulyuz, S.; Kiskan, B. Combination of polyethylenimine and vanillin-based benzoxazine as a straightforward self-healable system with excellent film-forming ability. *Macromolecules* **2024**, *57*, 2078–2089. [[CrossRef](#)]
24. Periyasamy, T.; Asrafali, S.P.; Muthusamy, S. New benzoxazines containing polyhedral oligomeric silsesquioxane from eugenol, guaiacol and vanillin. *New J. Chem.* **2025**, *39*, 1691–1702. [[CrossRef](#)]
25. Appasamy, S.M.G.; Krishnasamy, B.; Ramachandran, S.; Muthukaruppan, A. Vanillin derived partially bio-based benzoxazine resins for hydrophobic coating and anticorrosion applications: Studies on syntheses and thermal behavior. *Polym. Plast. Tech. Mat.* **2023**, *63*, 287–298. [[CrossRef](#)]
26. Sini, N.K.; Bijwe, J.; Varma, I.K. Thermal behaviour of bisbenzoxazines derived from renewable feed stock vanillin. *Polym. Degrad. Stab.* **2024**, *109*, 270–277. [[CrossRef](#)]
27. Ye, J.; Lu, X.; Xin, Z. Cardanol-based polybenzoxazine coatings: Crosslinking structures, hydrophobicity and corrosion protection properties. *J. Polym. Sci.* **2024**, *62*, 2936–2944. [[CrossRef](#)]
28. Chen, X.; Zhang, X.; Chen, J.; Bai, W.; Zheng, X.; Lin, Q.; Lin, F.; Xu, Y. Two-dimensional lamellar polyimide/cardanol-based benzoxazine copper polymer composite coatings with excellent anti-corrosion performance. *RSC Adv.* **2022**, *12*, 10766–10777. [[CrossRef](#)]
29. Fan, Z.; Li, B.; Ren, D.; Xu, M. Recent progress of low dielectric and high-performance polybenzoxazine-based composites. *Polymers* **2023**, *15*, 3933. [[CrossRef](#)]
30. Anagwu, F.I.; Dossi, E.; Skordos, A.A. High glass transition catalyst-free polybenzoxazine vitrimer through one-pot solventless method. *React. Funct. Polym.* **2025**, *209*, 106186. [[CrossRef](#)]
31. Zhao, J.Q.; Liu, Y.; Zhang, S.M.; Qiu, J.J.; Liu, C.M. Bio-based, main-chain type polybenzoxazine precursor derived from sustainable furfurylamine and salicylaldehyde: Synthesis, characterization and properties. *React. Funct. Polym.* **2020**, *149*, 104516. [[CrossRef](#)]

32. Zhao, C.; Sun, Z.; Wei, J.; Li, Y.; Xiang, D.; Wu, Y.; Que, Y. A phosphorous-containing bio-based furfurylamine type benzoxazine and its application in bisphenol-A type benzoxazine resins: Preparation, thermal properties and flammability. *Polymers* **2022**, *14*, 1597. [[CrossRef](#)]
33. Periyasamy, T.; Asrafali, S.P.; Kim, S.C. Bio-based polybenzoxazine-cellulose grafted films: Material fabrication and properties. *Polymers* **2023**, *15*, 849. [[CrossRef](#)]
34. Derradji, M.; Khiari, K.; Mehelli, O.; Abdous, S.; Amri, B.; Belgacemi, R.; Ramdani, N.; Zegaoui, A.; Liu, W. Green composites from vanillin-based benzoxazine and silane surface modified chopped carbon fibers. *Polym. Renew. Resour.* **2023**, *14*, 16–30. [[CrossRef](#)]
35. Bessa, W.; Trache, D.; Ghalimi, C.; Aidi, S.; Tarchoun, A.F.; Gahfif, F.; Abdelaziz, A.; Thakur, S.; Hussin, M.H. Curing kinetics of composites based on benzoxazine resin and microcrystalline cellulose modified by phosphorus salt. *Thermochim. Acta* **2024**, *735*, 179718. [[CrossRef](#)]
36. Soudjrari, S.; Derradji, M.; Amri, B.; Djaber, K.; Mehelli, O.; Tazibet, S.; Abdous, S.; Ramdani, N.; Liu, W.; Khadraoui, A. Novel vanillin-based benzoxazine containing phthalonitrile thermosetting system: Simple synthesis, autocatalytic polymerization and high thermomechanical properties. *High Perform. Polym.* **2022**, *34*, 818–827. [[CrossRef](#)]
37. Mora, P.; Rimdusit, S.; Karagiannidis, P.; Srisorrachatr, U. Mechanical properties and curing kinetics of bio-based benzoxazine–epoxy copolymer for dental fiber post. *Bioresour. Bioprocess.* **2023**, *10*, 62. [[CrossRef](#)]
38. Prathumrat, P.; Tiptipakorn, S.; Rimdusit, S. Multiple-shape memory polymers from benzoxazine-urethane copolymers. *Smart Mater. Struct.* **2017**, *26*, 065025. [[CrossRef](#)]
39. Zhao, T.; Jiang, Z.; Ge, Y.; Yin, H.; Yang, Q.; Li, R.; Chen, Z.; Zhang, H.; Liu, X. Mechanical properties, biosafety, and shearing bonding strength of glass fiber–reinforced PEEK composites used as post-core materials. *J. Mech. Behav. Biomed. Mater.* **2023**, *145*, 106047. [[CrossRef](#)]
40. Assaf, J.; Hardan, L.; Kassis, C.; Bourgi, R.; Devoto, W.; Amm, E.; Moussa, C.; Sawicki, J.; Lukomska-Szymanska, M. Influence of resin cement thickness and elastic modulus on the stress distribution of zirconium dioxide inlay-bridge: 3D finite element analysis. *Polymers* **2021**, *13*, 3863. [[CrossRef](#)]
41. Wang, B.; Huang, M.; Dang, P.; Xie, J.; Zhang, X.; Yan, X. PEEK in fixed dental prostheses: Application and adhesion improvement. *Polymers* **2022**, *14*, 2323. [[CrossRef](#)]
42. Reynaldo, M.C.; Luzmila, V.R.; Flor, S.R.; Carlos, L.G.; Ana, A.M.; Rosa, A.A.; César, C.R. Adhesive strength of glass fiber-reinforced posts with silane conditioning versus universal adhesive system conditioning: An in vitro study. *J. Int. Oral Health* **2024**, *16*, 290–296.
43. Fuchs, F.; Mayer, L.A.; Unterschütz, L.; Ziebolz, D.; Oberueck, N.; Schulz-Kornas, E.; Hahnel, S.; Koenig, A. Effect of powder air polishing and ultrasonic scaling on the marginal and internal interface (tooth-veneer) of ceramic veneers: An in vitro study. *Clin. Oral. Investig.* **2024**, *28*, 655. [[CrossRef](#)]
44. Mora, P.; Rimdusit, S.; Jubsilp, C. Development, characteristics, and potential applications of green composites from bio-derived polybenzoxazine and glass fiber. *Polym. Compos.* **2025**. [[CrossRef](#)]
45. Wang, Y.; Wang, S.; Meng, Y.; Liu, Z.; Li, D.; Bai, Y.; Yuan, G.; Wang, Y.; Zhang, X.; Li, X.; et al. Pyro-catalysis for tooth whitening via oral temperature fluctuation. *Nat. Commun.* **2022**, *13*, 4419. [[CrossRef](#)] [[PubMed](#)]
46. Huidan Wei, H.; Wu, Q.; Zhao, X.; Chen, K.; Sun, J.; Cui, Z.; Wang, C. Preparation and characterization of luminescent polyimide/glass composite fiber. *J. Mater. Res. Technol.* **2022**, *18*, 4329–4339.
47. ASTM D 792-20; American Society for Testing and Materials (ASTM D 792-20) Standard Test Methods for Density and Specific Gravity (Relative Density) of Plastics by Displacement. International ASTM: West Conshohocken, PA, USA, 2020.
48. ASTM D 790M-93; American Society for Testing and Materials (ASTM D 790M-93) Standard Test Methods for Flexural Properties of Unreinforced and Reinforced Plastics and Electrical Insulating Materials. International ASTM: West Conshohocken, PA, USA, 1993.
49. Pegoretti, A.; Fambri, L.; Zappini, G.; Bianchetti, M. Finite element analysis of a glass fibre reinforced composite endodontic post. *Biomaterials* **2002**, *23*, 2667–2682. [[CrossRef](#)]

Disclaimer/Publisher’s Note: The statements, opinions and data contained in all publications are solely those of the individual author(s) and contributor(s) and not of MDPI and/or the editor(s). MDPI and/or the editor(s) disclaim responsibility for any injury to people or property resulting from any ideas, methods, instructions or products referred to in the content.